Path Loss Exponent Estimation in Large Wireless Networks

Sunil Srinivasa and Martin Haenggi
Department of Electrical Engineering
University of Notre Dame
Notre Dame, IN 46556, USA
Email: {*ssriniv1, mhaenggi*}*@nd.edu*

Abstract

Even though the analyses in many wireless networking problems assume that the value of the path loss exponent (PLE) is known a priori, this is often not the case, and an accurate estimate is crucial for the study and design of wireless systems. In this paper, we address the problem of estimating the PLE in large wireless networks, which is relevant to several important issues in communications such as localization, energy-efficient routing, and channel access. We consider a large ad hoc network where nodes are distributed as a homogeneous Poisson point process on the plane, and the channels are subject to Nakagami-m fading. We propose and discuss three algorithms for PLE estimation under these settings that explicitly take into account the interference in the network. Simulation results are provided to demonstrate the performance of the algorithms and quantify the estimation errors.

Index Terms

Wireless networks, path loss exponent, estimation, Crámer-Rao lower bound, Poisson point process, interference, Nakagami-m fading.

I. Introduction

The wireless channel presents a formidable challenge as a medium for reliable high-rate communication. It is responsible not only for the attenuation of the propagated signal but also causes unpredictable spatial and temporal variations in this loss due to user movement and changes in the environment. In order to capture all these effects, the path loss for RF signals is commonly represented as the product of a deterministic distance component (large-scale path loss) and a randomly-varying component (small-scale fading) [1]. The large-scale path loss model assumes that the received signal strength falls off with distance according to a power law, at a rate termed the path loss exponent (PLE). Fading describes the fluctuations in the received signal strength due to the constructive and destructive addition of its multipath components. While variations due to path loss happen over large distances (hundreds of meters), variations due to multipath occur over much shorter distances, on the order of the RF wavelength. The large-scale path loss is one of the simplest model for signal propagation and a major component considered during the analysis and design of communication systems [2]. An critical issue is to characterize the large-scale behavior of the channel and accurately estimate the PLE, based solely on received signal measurements.

This problem is not trivially solvable even for a single link due to the existence of multipath propagation and thermal noise. For large ad hoc and sensor networks, the problem is further complicated due to the following reasons: First, the achievable performance of a typical wireless network is not only susceptible to noise and fading, but also to interference due to the presence of simultaneous transmitters. Dealing with fading and interference simultaneously is a major difficulty in the estimation problem. Moreover, the distances between nodes are subject to uncertainty. Often, the distribution of the underlying point process can be statistically determined, but precise locations of the nodes are harder to measure. In such cases, we will need to consider the fading and distance ambiguities jointly, i.e., define a spatial point process that incorporates both. In this paper, we present three different methods to accurately estimate the channel's PLE for large wireless networks in the presence of fading, noise and interference, based on the received signal strength measurements. We also provide simulation results to illustrate the performance of the algorithms and study the estimation error. Additionally, we furnish some basic methods to infer the intensity of the Poisson process, while providing Crámer-Rao lower bounds on the mean squared error (MSE) of the intensity estimates wherever possible.

The remainder of the paper is structured as follows. Section II provides a few examples to motivate the importance of knowing the PLE for analysis and design of communication systems and also discusses the prior work on the estimation problem. Section III presents the system and channel models. Section IV discusses the methods for estimating the intensity of the point process. Section V describes the algorithms for PLE estimation. Section VI compares the three PLE prediction algorithms, and Section VII concludes the paper.

II. Motivation and Related Work

A. Motivation

In this section, we illustrate the importance of knowing the PLE in the analysis and design of wireless networks. Though it is often assumed that the value of the PLE is known a priori, this is not true in practice, and an accurate estimate of the PLE is crucial for solving them.

The problem of PLE estimation is closely related to that of localization and can essentially be thought of as its complementary problem. In sensor networks, node localization is an integral component of network self-configuration. When bestowed with the ability to detect their positions, ad hoc deployed sensor nodes can support a rich set of geographically aware protocols and accurately report the regions of detected events. Detailed knowledge of the nodes' locations is also needed for performing energy-efficient routing in a decentralized fashion. An important class of localization algorithms are the ones based on received signal strength (RSS) measurements [3], [4] that need accurate estimates of the PLE to perform well. Another fundamental issue in wireless sensor networks is the sensing problem that deals with how well and accurately a target area or a phenomenon can be monitored. Of importance in such applications are characteristics such as the coverage and the connectivity of the network, and studying these properties need accurate estimates of the PLE [5], [6].

Many of the existing results on capacity scaling for large ad hoc networks strongly depend on the PLE as well. With γ being the PLE, the best known achievability result [7] states that for a network having n uniformly randomly located nodes, the capacity scales as $n^{2-\gamma/2}$ for $2 \leq \gamma < 3$ and as $\sqrt{n}$ for $\gamma \geq 3$. Depending on the value of the PLE, appropriate routing strategies (nearest-neighbor hopping or hierarchical cooperative schemes) may be implemented to reach the maximally achievable scaling of the system throughput. A good knowledge of the PLE is also essential for designing simple line networks. [8] discusses capacity results for TDMA-based linear networks and shows that the optimum number of hops to achieve a desired end-to-end rate strongly depends on the PLE. For example, when the desired (bandwidth-normalized) spectral efficiency exceeds the PLE, single-hop transmission outperforms multihopping.

Energy consumption in wireless networks is a crucial issue that needs to be addressed at all the layers of the communication system. [9] analyzes the energy consumed for several routing strategies that employ hops of different lengths in a large network with uniformly randomly distributed nodes. Using the results therein, we demonstrate that a good knowledge of the PLE is necessary for efficient routing. Consider the following two simple schemes where communication is assumed to occur only in a sector ϕ around the source-destination axis.

1) Route across n nearest neighbor hops in a sector ϕ, i.e., the next-hop node is the nearest neighbor that lies within $\pm\phi/2$ of the axis to the destination.
2) Transmit directly to the n'th neighbor in the sector ϕ. Here, n' is chosen in a way that the expected progress

is the same for both schemes.

From [9], the ratio of the consumed energies for the two schemes is obtained as

$$\frac{E_1}{E_2} = \frac{n^2\Gamma(1+\gamma/2)\Gamma(n')}{\Gamma(n'+\gamma/2)},$$

where $\Gamma(.)$ represents the Gamma function and $n' = \frac{\pi}{4}(n^2-1)+1$. We see that the PLE plays an important role in determining energy-efficient routing strategies. When γ is small, scheme 2 consumes less energy while relaying is beneficial at high PLE values.

The performance of contention-based systems such as slotted ALOHA is very sensitive to the contention probability p, hence it is critical to choose the optimal operating point of the system. The value of the contention parameter is determined based on various motives such as maximizing the network throughput [10, Eqn. 20] or optimizing the spatial density of progress [11, Eqn. 5.6]. These quantities also greatly depend on the PLE, and therefore the optimal value of the contention probability can be chosen only after estimating γ.

PLE estimation is also an integral component of the cellular phone location system, which has garnered considerable attention. There are several reasons why network providers need to estimate the position of mobile terminals in the network. Primarily, they have to be able to assist emergency communications, which needs accurate location estimates of the mobiles. Localization is also desired to provide positioning, tracking and navigation services to people with special needs, such as firefighters, soldiers, elderly patients, etc. Besides, knowing the PLE helps to accurately determine when the handoff procedure needs to be initiated so that calls are not dropped. In addition, it helps carry out open loop power control efficiently.

B. Review of Literature

In this section, we survey some of the existing PLE estimation methods in literature. Most authors have assumed a simplified channel model consisting only of a large-scale path loss component and a shadowing counterpart, but we are not aware of any prior work that has considered fading and interference jointly in the system model. Therefore, much of the past work on PLE prediction has focused mainly on RSS-based localization techniques. However, we remark that ignoring interference in the system model is not realistic, in particular since PLE estimation needs to be performed even before the network is organized.

Estimation based on a known internode distance probability distribution is discussed in [12]. The authors assume that the distance distribution between two neighboring nodes i and j is known or can be determined easily. With the transmit power equal to P_0[dBm] (assume this is a constant for all nodes), the RSS at node j is modeled by a log-normal behavior as

$$P_{ij}[\text{dBm}] \sim \mathcal{N}(\overline{P}_{ij}[\text{dBm}], \sigma^2_{\text{dB}}),$$

where σ denotes the log-normal spread and $\overline{P}_{ij}[\text{dBm}] = P_0[\text{dBm}] - 10\gamma \log_{10} d_{ij}$. Now, if the neighbor's distance distribution is given by $p_R(r)$, then

$$\overline{P}_{ij} = P_0 \mathbb{E}_R \left[R^{-\gamma} \right]. \tag{1}$$

E.g., if the internodal distance distribution is Rayleigh[1] with mean $\sqrt{\pi/2}$, then

$$\overline{P}_{ij} = P_0 2^{-\gamma/2} \Gamma(1 - \gamma/2). \tag{2}$$

The value of γ is obtained by equating $\overline{P}_{ij}$ to the empirical mean value of the received powers taken over several node pairs i and j.

If the nearest neighbor distribution is in a complicated form that is not integrable, an idea similar to the quantile-quantile plot can be used [12]. For cases where it might not be possible to obtain the neighbor distance distribution, the idea of estimating γ using the concept of the Cayley-Menger determinant or the pattern matching technique [12] is useful.

As described earlier, the situation is completely different when interference and fading are accounted for and we cannot use the commonly known RSS-based estimators directly.

III. System Model

We consider a large planar ad hoc network, where nodes are distributed as a homogeneous Poisson point process (PPP) Φ of intensity λ (assumed unknown). Therefore, given a Borel set B, the number of points lying in it, denoted by $\Phi(B)$, is Poisson-distributed with mean $\lambda \nu_2(B)$, where $\nu_2(\cdot)$ is the two-dimensional Lebesgue measure (area). Also, the number of points in disjoint sets are independent random variables. The PPP model for the nodal distribution is a ubiquitously used one and may be justified by claiming that sensor nodes are dropped from an aircraft in large numbers; for mobile ad hoc networks, it may be argued that terminals move independently of each other.

The attenuation in the channel is modeled as a product of the large-scale path loss with exponent γ and a flat block-fading component. To obtain a concrete set of results, the amplitude H is taken to be Nakagami-m distributed. Letting $m = 1$ results in the well-known case of Rayleigh fading, while lower and higher values of m signify stronger and weaker fading scenarios respectively. $m \to \infty$ can be used to study the case of no fading. The block fading assumption is necessary for our analysis and may be justified by assuming that the nodes or surrounding objects move slightly so that in each transmission block, different fading realizations are observed. When dealing with received signal powers, we use the power fading variable denoted by $G = H^2$. Since G captures

[1]The nearest neighbor distance function when the nodal arrangement is a planar Poisson point process (PPP) is Rayleigh distributed [9]. The mean value assumed is just for the sake of convenience.

the random deviation from the large-scale path loss, $\mathbb{E}_G[G] = 1$. The moments of G are [13]

$$\mathbb{E}_G[G^n] = \frac{\Gamma(m+n)}{m^n \Gamma(m)},$$

and the variance is $\sigma_G^2(G) = 1/m$.

Since the PLE estimation is usually performed during network initialization, it is fair to assume that the transmissions in the system during this phase are uncoordinated. Therefore, we take the channel access scheme to be ALOHA. However, for analytical tractability, we assume that transmissions occurs in time slots. We denote the slotted ALOHA contention probability by a constant p. Consequently, the set of transmitters forms a PPP Φ' of intensity λp. Also, we assume that all the transmit powers are equal to unity. Then, the interference at node y on the plane is given by

$$I_\Phi(y) = \sum_{z \in \Phi'} G_{zy} \|z - y\|^{-\gamma},$$

where g_{zy} is the fading gain of the channel and $\|\cdot\|$ denotes the Euclidean distance.

We say that communication from the transmitter at x to the receiver at y is successful if and only if the signal-to-noise and interference ratio (SINR) at y is larger than a threshold Θ, which depends on the modulation and coding scheme and the receiver structure. Mathematically speaking, an outage occurs if and only if

$$\frac{G_{xy}\|x - y\|^{-\gamma}}{N_0 + I_{\Phi' \setminus \{x\}}(y)} < \Theta, \tag{3}$$

where $I_{\Phi \setminus \{x\}}(y)$ denotes the interference in the network at y due to all the transmitters, except the desired one at x, and N_0 is the noise power.

IV. Estimation of the density of the Poisson network

First, we furnish some basic methods to estimate the intensity of the network, which will be useful in the later sections of the paper to estimate not only the PLE but also the parameters p and m. We also analyze Crámer-Rao lower bounds on the MSE wherever possible.

A. The Naive Solution

The most fundamental method to estimate the network's intensity is simply to use its definition. Observing the process through a 2D-window W, an unbiased estimator for the intensity is given by

$$\hat{\lambda} = \Phi(W)/\nu_2(W). \tag{4}$$

We know that $\Phi(W)$ is Poisson-distributed with mean $\lambda\nu_2(W)$ i.e., it is governed by a probability mass function

$$f(\Phi(W) = k; \lambda) = \exp(-\lambda\nu_2(W))\frac{(\lambda\nu_2(W))^k}{k!}. \tag{5}$$

The regularity condition is met in this case [14]

$$\frac{\partial}{\partial\lambda}\ln f(\Phi(W) = k; \lambda) = \frac{\nu_2(W)}{\lambda}\left[\hat{\lambda} - \lambda\right], \tag{6}$$

and thus, this is an efficient estimator meeting the following Crámer-Rao lower bound (CRLB) on the error variance:

$$\text{MSE}(\hat{\lambda}) = \lambda/\nu_2(W). \tag{7}$$

Since Φ is ergodic, $\hat{\lambda}$ is strongly consistent in the sense that it almost surely converges to the true value i.e., $\hat{\lambda} \to \lambda$ as the window's area is increased. Table I consists of recorded estimates for a sample network realization and supports the fact that the estimation error reduces as the window size is made large. The theoretic MSE values are also provided.

TABLE I
$\hat{\lambda}$ FOR VARIOUS CIRCULAR WINDOW SIZES. TRUE VALUE: $\lambda = 1$.

Window radius	25	50	75	100	200
Estimate of λ	0.9841	1.0339	1.0227	1.0190	1.0085
% Error	-1.59	3.39	2.27	1.9	0.85
MSE	5.1e-4	1.27e-4	5.7e-5	3.2e-5	8e-6

Once λ has been roughly estimated, confidence intervals can be established [15]. Crow et al. provide approximate confidence intervals for λ, employing the normal approximation and a continuity correction [16]. If δ be the desired breadth of the confidence interval and ϵ the required confidence level, then

$$\delta\nu_2(W) \approx \left[\frac{z_{\epsilon/2}}{2} + \sqrt{1 + \lambda\nu_2(W)}\right]^2 - \left[\frac{z_{\epsilon/2}}{2} - \sqrt{\lambda\nu_2(W)}\right]^2, \tag{8}$$

where $z_{\epsilon/2} = \text{Q}^{-1}(\epsilon/2)$, and $\text{Q}^{-1}(\cdot)$ is the inverse Q-function. From this, we can use the preliminary estimate of λ to obtain

$$\nu_2(W) \approx \frac{4z_{\epsilon/2}^2\lambda}{\delta^2}. \tag{9}$$

Accordingly, if one wishes to obtain an estimate of the intensity accurate to 2 decimal places ($\delta = 0.01$) with 99% confidence ($\epsilon = 0.01$), and a preliminary estimate of $\lambda = 1$, $\nu_2(W) = 266256$. A square of side about 500 units is needed to obtain an accurate estimate.

Alternatively, one can observe the process through N disjoint windows $W_1, \ldots, W_N$ and use the unbiased

estimator

$$\hat{\lambda} = \frac{1}{n} \sum_{i=1}^{N} \frac{\Phi(W_i)}{\nu_2(W_i)}. \tag{10}$$

However, for nodes to be able to make these measurements, they need to have knowledge of their locations and also the window boundaries. Since $\Phi(W_i)$ are independent random variables for each i, the following Crámer-Rao bound is established on the MSE.

$$\text{MSE}(\hat{\lambda}) \geq \frac{\lambda}{\sum_{i=1}^{N} \nu_2(W_i)}. \tag{11}$$

Since this meets the regularity condition and is the minimum variance unbiased estimator, it is also the maximum-likelihood estimator. As a large number of windows are considered, the MSE vanishes. Also, if the window size is large, the MSE is nulled as seen before.

B. Estimation Based on Empty Quadrats

Here, the observation window W is partitioned into a large number of disjoint square subregions each of equal area a^2. The void probability for the PPP in each of those small quadrats is equal to $p_0 = \exp(-\lambda a^2)$. Equating the fraction of empty quadrats to p_0, λ is estimated as

$$\hat{\lambda} = \ln(1/p_0)/a^2. \tag{12}$$

The estimates of the intensity for a sample realization of the PPP are shown in Table II. To obtain these estimates, we generated a PPP with unit intensity on a 150×150 square window and used quadrats of size $a \times a$. The smaller a, the more accurate is the estimate, since it is based on more quadrats, which permits better averaging. Note that this method can also be performed with subregions of equal area that are not necessarily squares.

TABLE II
$\hat{\lambda}$ USING THE EMPTY QUADRATS METHOD. TRUE VALUE OF $\lambda = 1$.

a	2	1	0.5	0.25
$\hat{\lambda}$	1.0366	1.0055	0.9979	0.9994
% Error	3.66	0.55	-0.21	-0.06

C. Estimation Based on Nearest Neighbor Distances

In certain situations, it might be possible to measure distances between nodes in the network. One such case is where the location of some nodes are known and these act as beacons assisting other nodes to estimate their locations. The knowledge of the nearest neighbor distances can be used to assist in estimating the network's intensity.

In a homogeneous Poisson network, it is well-known that the neighbor distances follow a generalized gamma distribution [17]. Accordingly, the density of the distance to the k^{th}-nearest neighbor for a planar network is given

by

$$f(d_k = r; \lambda) = \exp(-\lambda\pi r^2)\frac{2(\lambda\pi r^2)^k}{r\Gamma(k)}, \quad k = 1, 2, \ldots. \tag{13}$$

The maximum-likelihood (ML) estimate of λ is obtained from here by setting [14]

$$\frac{\partial}{\partial\lambda} f(d_k = r; \lambda)|_{\lambda=\hat{\lambda}_{\text{ML}}} = 0,$$

which gives

$$\hat{\lambda}_{\text{ML}} = k/\pi r^2. \tag{14}$$

For a more accurate result, we can use N beacon nodes to make a N-sized vector measurement, resulting in the ML estimate

$$\hat{\lambda}_{\text{ML}} = \frac{Nk}{\pi \sum_{i=1}^{N} r_i^2}. \tag{15}$$

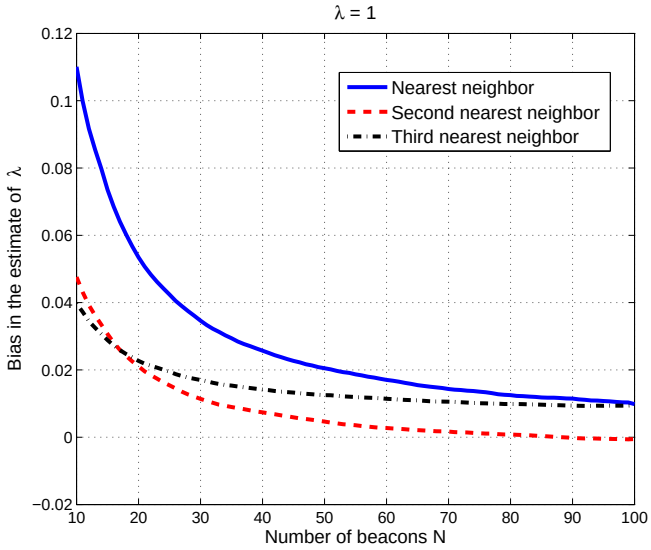

Fig. 1. The bias in $\hat{\lambda}_{\text{ML}}$ for the k^{th} nearest neighbor measurements captured from N beacons for $k = 1, 2, 3$.

However, as Fig. 1 depicts, the ML estimate is biased. Moreover, the bias takes on negative values as well. The CRLB for an unbiased estimate of λ is given by the inverse of the Fisher information as

$$\begin{aligned} \text{CRLB} &= \frac{1}{\mathbb{E}_R\left[\frac{\partial^2}{\partial\lambda^2}\ln f(R;\lambda)\right]} \\ &= \frac{\lambda^2}{kN}. \end{aligned} \tag{16}$$

Fig. 2 plots the MSE and the CRLB for the estimates obtained from the first three neighbors' distance measurements. Though it is seen that the estimation error is lowered with farther neighbors, it is harder to make such

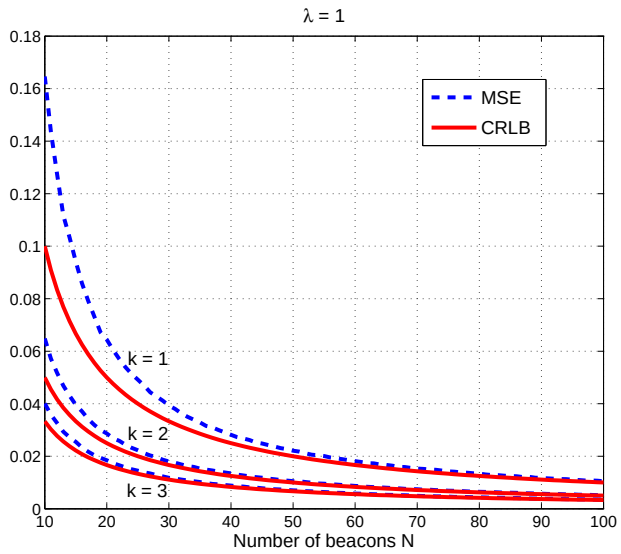

Fig. 2. The MSE of $\hat{\lambda}$ against the CRLB for the k^{th} nearest neighbor measurements captured from N beacons for $k = 1, 2, 3$.

measurements since it requires information to be relayed across more nodes.

V. Path Loss Exponent Estimation

This section describes three algorithms for PLE estimation and also provides simulation results on the estimation errors. Each method is based on a certain network characteristic namely the interference moments, the outage probabilities and the network's connectivity properties, respectively. The PLE estimation problem is essentially tackled by equating the practically measured values of these quantities to the theoretically established ones to obtain $\hat{\gamma}$. There is a caveat though, that needs to be addressed. In theory, we assume that we have access to a large number of realizations and usually derive results for an "average network", that is the one obtained by averaging over all possible realizations of the nodal distributions and channels. However, the problem in practice is that we have only a single realization of the nodal distribution at hand. Fortunately, in the scenario where nodes are distributed as a homogeneous PPP, we can work around this issue by using its property of ergodicity. We now state the ergodic theorem for spatial processes that states that statistical averages of measurable functions may be replaced by spatial averages. Using this, we argue that a single realization of the network is sufficient for accurate estimation of the PLE.

Theorem 5.1: (Ergodic Theorem [15, p. 172]) Let $T : X \to X$ be a measure-preserving ergodic transformation on a measure space (X, Σ, ν) and consider a "well-behaved" function [2]. Define the "time-average" of f, $\hat{f}(x)$ as

[2]More precisely, f must be L^1-integrable w.r.t the measure ν i.e., $f \in L^1(X, \Sigma, \nu)$.

the average over iterations of T starting at some initial point x. Accordingly,

$$\hat{f}(x) = \lim_{n\to\infty} \frac{1}{n} \sum_{k=0}^{n-1} f(T^k x), \tag{17}$$

where T^k is the k^{th} iterate of T. Likewise, the spatial average of f is defined as

$$\bar{f}(x) = \frac{1}{\nu(X)} \int f d\nu. \tag{18}$$

Assuming that $\nu(X)$ is nonzero and finite, $\hat{f}(x) = \bar{f}(x)$ almost everywhere.

The ergodic theorem states that for an ergodic endomorphism, the space and time averages are equal almost everywhere. Let T denote the transformation whose iterates result in different realizations of the PPP. Since the PPP is ergodic, T represents a measure-preserving ergodic transformation. Thus, while $\hat{f}(x)$ reflects the average of f over different realizations of the PPP at a single node, $\bar{f}(x)$ is equivalent to taking an average over different nodes in a single realization, and these two are equal almost everywhere. In conclusion, we remark that the estimation process can be performed in practice by looking only at a single realization of the network and taking the necessary measurements over several nodes.

Throughout this paper, simulation results were obtained using MATLAB. The PPP was generated by distributing a Poisson number of points uniformly randomly in a 150×150 square with density 1. However, in order to avoid border effects, only the nodes lying inside the inner 120×120 square were chosen for measurements. For analyzing the error performance of the algorithms, we used estimates resulting from a million different realizations of the PPP.

A. Estimation Using the Moments of the Interference

A simple technique to infer the PLE γ uses the knowledge of the interference moments. Using the estimation value of the PLE and the predicted value of the intensity of the Poisson process (from the previous section), we can also infer the parameters p and m.

According to this method, nodes simply need to record the strength of the interference power that they observe. By the ergodic theorem, the mean and variance of the set of measurements at several different nodes match the theoretically determined values. We first state existing theoretic results and subsequently describe how the estimation can be performed in practice.

For the PPP network running the slotted ALOHA protocol, the n^{th} cumulants of the interference resulting from transmitters in an annulus of inner radius A and outer radius B around the receiver node are given as [18]

$$C_n = 2\pi\lambda p \mathbb{E}_G[G^n] \frac{B^{2-n\gamma} - A^{2-n\gamma}}{2 - n\gamma}. \tag{19}$$

In particular, we can consider only the case $\gamma > 2$ (a fair assumption in a wireless scenario) and let B to be large (considering the entire network) so that the mean and variance of the interference are

$$\mu_I = C_1 = 2\pi\lambda p \frac{A^{2-\gamma}}{\gamma - 2} \tag{20}$$

and

$$\sigma_I^2 = C_2 = 2\pi\lambda p \left(1 + \frac{1}{m}\right) \frac{A^{2-2\gamma}}{2\gamma - 2}. \tag{21}$$

Note that (19) states that all the moments of the interference are infinite for $A = 0$. However, the large-scale path loss model is valid only in the far-field of the antenna and breaks down for very small distances. Denote the (known) near-field radius by a positive constant A_0. The algorithm based on the interference moments works by matching the practical and theoretic values of the mean interference and is described as follows.

- Consider an arbitrary node in the network and number it node 1. Record the value of the interference power (received power) at node 1, I_1.
- Repeat the above method for several other nodes $(2, \ldots)$ recording values of interference powers $I_2, \ldots$ at the respective nodes. Eventually, the empirical mean interference $(1/N)\sum_{i=1}^{N} I_i$ averaged over N nodes converges.

By the ergodic theorem, the observed mean value matches the one given by (20) with $A = A_0$. The value of γ can be estimated by using a look-up table and the known values of p and estimated intensity $\hat{\lambda}$.

Alternatively, we can use a "differential method" that is based on measurements taken for two different guard zone radii values. A guard zone is the region around a node inside which there cannot be any transmitters. This algorithm assumes that each node has information on its location and creating guard zones is feasible. Basically, one needs to measure the mean interference values μ_I^1 and μ_I^2 for guard zone radii A_1 and A_2 respectively. Since these observed values of the mean interference match the theoretic values closely, we obtain

$$\frac{\mu_I^1}{\mu_I^2} = \left(\frac{A_1}{A_2}\right)^{2-\gamma},$$

and an unbiased estimate of γ is

$$\hat{\gamma} = 2 - \frac{\ln(\mu_I^1/\mu_I^2)}{\ln(A_1/A_2)}. \tag{22}$$

The advantage of the differential method is that it does not require the knowledge of the ALOHA contention probability p or the intensity of the process.

Fig. 3 depicts a stem plot of the histogram of the estimated PLE values. The predicted values fit well into a Gaussian curve (solid line) with the same statistics as the estimates, meaning that the estimation error is approximately Gaussian in nature. The estimate of γ is also seen to closely match its true value of 4.

The estimate $\hat{\gamma}$ can be used along with $\hat{\lambda}$ to predict the value of the transmission probability p (when it is

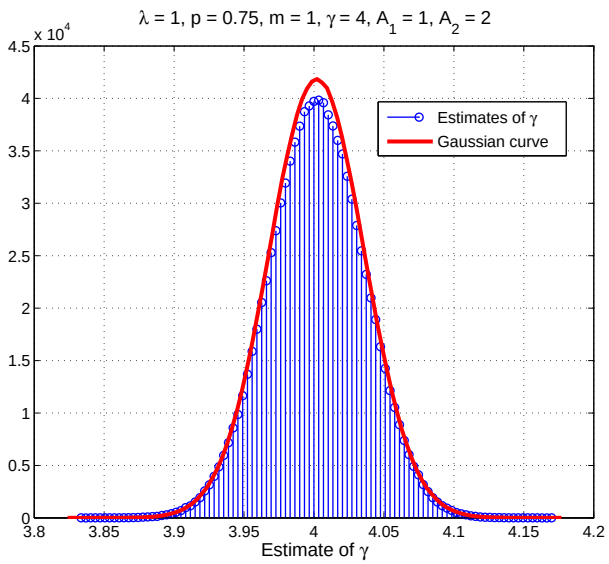

Fig. 3. Histogram of $\hat{\gamma}$ for the estimation algorithm based on the interference moments. Error variance ≈ 0.0015.

unknown). Indeed, using (20), an estimate of the ALOHA contention parameter is obtained immediately as

$$\hat{p} = \frac{\mu_I^1(\hat{\gamma}-2)}{2\pi\hat{\lambda}A_1^{2-\gamma}}. \tag{23}$$

Furthermore, an estimate of the fading parameter m is obtained by inverting (21) as

$$\hat{m} = \left(\frac{\sigma_I^2(\hat{\gamma}-1)}{\pi\hat{\lambda}\hat{p}A_1^{2-2\hat{\gamma}}} - 1\right)^{-1}, \tag{24}$$

where σ_I^2 is the empirical variance of the interference for guard zone radius A_1.

For the case that the channels are Rayleigh-faded (exponential received powers), we formulate two other schemes for the estimation process. The first method is based on outage probabilities, while another technique makes use of the connectivity properties of the network.

B. Estimation Based on Outage Probabilities

In the estimation procedure using the moments of the interference, a suitable guard zone needs to be imposed around each receiver node. This might not be a practical/feasible solution, particularly in cases where there is no relative node location information available. When it is known that the channel fading is Rayleigh, the PLE can also be estimated using outage probabilities as discussed below. Similar to the previous algorithm, here too, we do not need an estimate of λ or the value of p. We first derive some theoretic results and then describe a practical scheme to estimate γ.

By Slivnyak's theorem [15], the distribution of the PPP is unaffected by the addition of a point to the process but removing it from consideration. The introduction of this point is useful in formalizing the notion of a "typical

point" of the process. Given this, consider an arbitrary node in the network and in addition, place a transmitter at unit distance away from it[3]. Now, we shift the transmitter node to the origin and consider the outage probability for this typical node pair. The probability of success for this transceiver pair is given by

$$\begin{aligned} p_s &= \mathbb{E}_I^{!0}\left[\Pr(G > (N_0 + I)\Theta \mid I)\right] \\ &= \exp(-N_0\Theta)\mathbb{E}_I^{!0}\left[\exp\left(-I\Theta\right)\right] \\ &= \exp(-N_0\Theta)M_I\left(\Theta\right), \end{aligned} \tag{25}$$

where $M_I(s)$ is the moment generating function (MGF) of the interference power I and $\mathbb{E}_I^{!0}$ denotes the expectation with respect to the reduced Palm measure [15]. It is basically the expectation conditioned on there being a point at the origin 0, but not including the point for calculation of the interference power. Using the closed-form expression for the MGF [18, Eqn. 20], we have for $\gamma > 2$,

$$p_s = c_1 \exp(-c_2), \tag{26}$$

where $c_1 = \exp(-N_0\Theta)$ and $c_2 = \lambda p\pi\Gamma\left(1 + 2/\gamma\right)\Gamma\left(1 - 2/\gamma\right)\Theta^{2/\gamma}$. The outage probability $1 - p_s$ is plotted versus γ in Fig. 4 for different values of threshold.

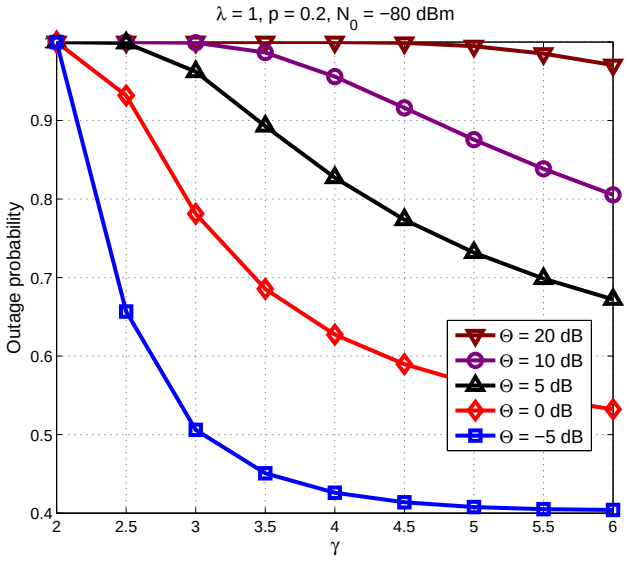

Fig. 4. Theoretical values of the outage probabilities at different thresholds.

For the rest of this subsection, we assume that the system is interference-limited. In other words, $N_0 \ll I$ and therefore, $p_s \approx \exp(-c_2)$. We now describe a practical scheme to estimate γ. The idea behind this algorithm is to compute the SIR values at each node and use the empirical distribution to compute the success probability, which

[3]The distance requirement is just a convenient assumption so that when the transceivers are unit distance apart, the PLE will not affect the received power strength

by the ergodic theorem, matches the theoretic value. It works as follows.

- Consider an arbitrary node, call it the receiving node and place a transmitter at a unit distance away from it. The transmitter should not belong to the original process. With a transmit power of unity, the received power due to that transmitter alone is exponential with unit mean. Measure the SIR at this receiver node.
- Repeat for several nodes, thus obtaining a histogram of the measured SIR values. For any given value of Θ, the probability of success can be empirically determined from the histogram.

The success probability obtained thus matches the one given by (26). If it is possible to measure the value of p, a look-up table can be generated to estimate the PLE using the known value of p and estimated intensity $\hat{\lambda}$.

If the density of the network or p is not accurately known, we can use a differential method to estimate γ. Accordingly, obtain histograms of the measured SINR for two different values of the threshold, say Θ_1 and Θ_2. Denote the empirical values of the success probabilities corresponding to the two values of Θ as p_s^1 and p_s^2. Theoretically, we obtain

$$\frac{\ln(p_s^1)}{\ln(p_s^2)} = \frac{\ln(M_I(\Theta_1))}{\ln(M_I(\Theta_2))} = \left(\frac{\Theta_1}{\Theta_2}\right)^{2/\gamma},$$

and therefore an unbiased estimate of γ is

$$\hat{\gamma} = \frac{2\ln(\Theta_1/\Theta_2)}{\ln(\ln(p_s^1)/\ln(p_s^2))}. \tag{27}$$

Fig. 5 plots the histogram of the estimated PLE values when the true value is $\gamma = 4$. The estimation error fits well into a Gaussian curve for this scheme as well.

We remark that it may not seem practical to place the transmitter for each receiver node where measurements are taken. Instead, nodes can equivalently assume the existence of a virtual transmitter and assume the signal power to be an exponential random variable with unit mean. This way, they can simply measure the interference power alone and compute the SIR.

a) Error analysis when the fading distribution is not necessarily Rayleigh: A critical assumption used for the estimation algorithm based on outage probabilities is that the fading component of the channel is Rayleigh distributed. It is interesting to see how the Nakagami fading parameter m affects the estimation results, i.e., how large the error is in the case that the fading distribution is not actually Rayleigh, but assumed to be so. We now provide some empirical results to depict the behavior of the error when the true value of m is not unity.

Fig. 6 shows the CDF of the error for some values of m ranging from 0.5 to ∞. For a slight deviation of m from unity, the predicted values differ largely from the true value, particularly when the fading effect is stronger than Rayleigh fading ($0.5 \leq m < 1$). The dotted line for $m = 1$ shows that the error median in this case is 0. Moreover, since the error is roughly Gaussian distributed, we verify that the estimate of γ is indeed unbiased when

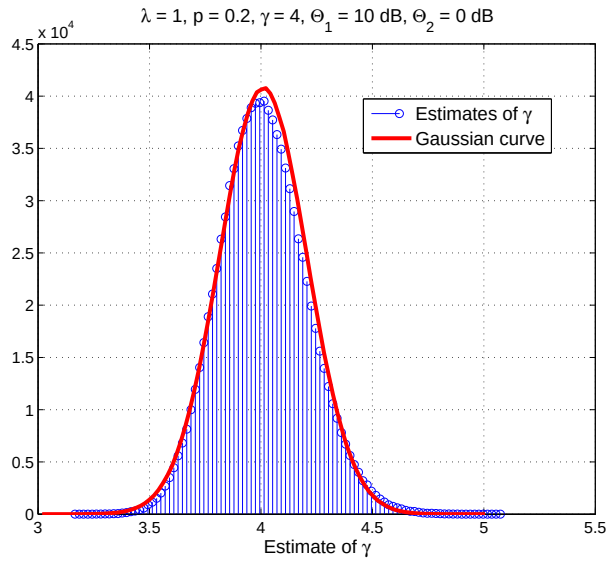

Fig. 5. Histogram of $\hat{\gamma}$ for the method based on outage probabilities. Error variance ≈ 0.04.

the channel is Rayleigh. We also observe that the error CDF converges as $m \to \infty$.

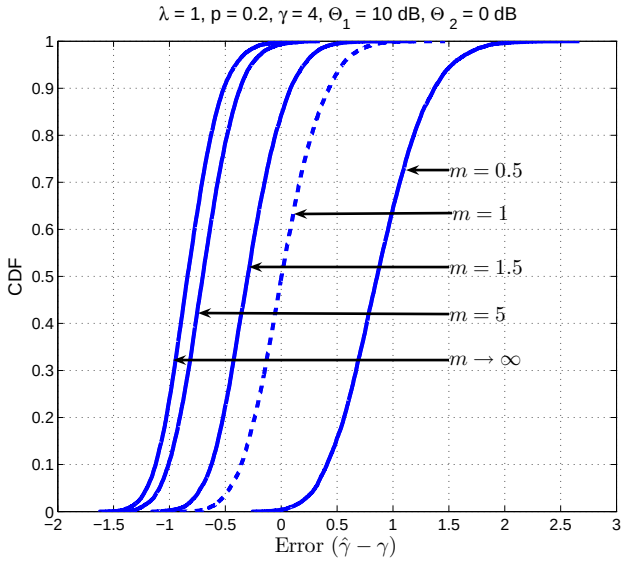

Fig. 6. CDF of the error $\hat{\gamma} - \gamma$.

Fig. 7 plots the MSE, taken over several different network realizations versus m for different PLE values. Again, we observe that the performance of this algorithm depends critically on the fading parameter m especially at lower values, since a slight deviation of m from unity largely affects the estimation error.

As a supplement to this subsection, we now analytically derive the outage probability when the fading component G is a general Nakagami-m distributed variable.

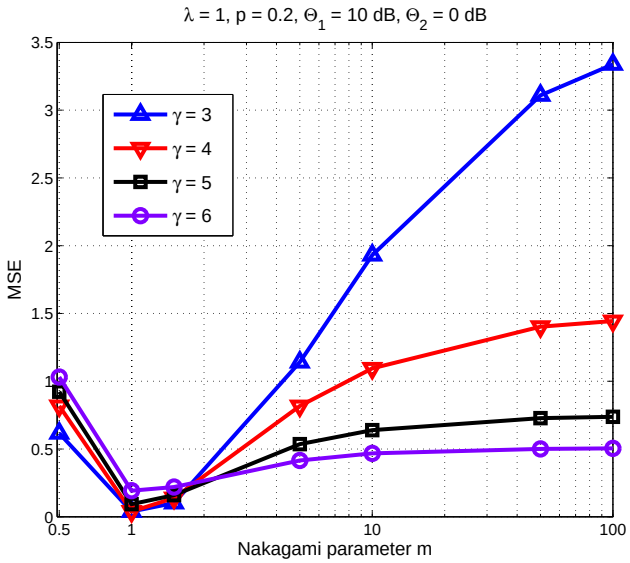

Fig. 7. The value of the MSE versus m for different PLEs.

The pdf of the power fading variable is given by

$$p_G(x) = \frac{m^m}{\Gamma(m)} x^{m-1} \exp(-mx), \quad m \geq 0.5. \tag{28}$$

Using this, we have

$$\begin{aligned} p_s &= \mathbb{E}_I^{!0}\left[\Pr(G > I\Theta \mid I)\right] \\ &= \mathbb{E}_I^{!0}\left[\int_{I\Theta}^{\infty} \frac{m^m}{\Gamma(m)} x^{m-1} \exp(-mx) dx\right] \\ &= \frac{1}{\Gamma(m)} \int_0^{\infty} \Gamma(m, x\Theta m) P_I(x) dx, \end{aligned} \tag{29}$$

where $\Gamma(\cdot,\cdot)$ is the upper incomplete gamma function[4] and $P_I(x)$ denotes the pdf of the interference function.

The expressions can be further simplified when m is an integer. For $m \in \mathbb{Z}^+$, we have

$$\begin{aligned} p_s &\overset{(a)}{=} \sum_{k=0}^{m-1} \frac{1}{k!} \int_0^{\infty} (x\Theta m)^k \exp(-x\Theta m) P_I(x) dx \\ &\overset{(b)}{=} \sum_{k=0}^{m-1} \frac{(-\Theta m)^k}{k!} \frac{d^k}{ds^k} M_I(s)|_{s=\Theta m}, \end{aligned} \tag{30}$$

where (a) is obtained from the series expansion of the upper incomplete gamma function and (b) from the definition of the MGF. We also have the following closed-form expression for the MGF [18, Eqn. 20]

$$M_I(s) = \exp(-\lambda p \pi \mathbb{E}_G[G^{2/\gamma}] \Gamma(1 - 2/\gamma) s^{2/\gamma}).$$

[4]Mathematica: Gamma[a,z]

Using this, we get

$$p_s = \exp(-c_3) \sum_{k=0}^{m-1} \frac{c_3^k}{k!} \left(\frac{2}{\gamma}\right)^k, \tag{31}$$

where $c_3 = \lambda p \pi \mathbb{E}_G(G^{2/\gamma})\Gamma(1-2/\gamma)(\Theta m)^{2/\gamma}$. The outage probabilities at integer values of m for $\gamma > 2$ can be numerically evaluated from the above equation.

C. Estimation Based on the Cardinality of the Transmitting Set

In this subsection, we present a method to estimate the PLE based on the connectivity properties of the network. For any node, define its transmitting set as the group of transmitting nodes whom it receives a packet from, in a given time slot. More formally, for receiver y, transmitter node x is in its transmitting set if they are connected i.e., the SINR at y is greater than a certain threshold Θ. Note that this set changes from time slot to time slot. This algorithm is based on matching the theoretic and practical values of the mean number of elements in the transmitting set. Note that for $\Theta = 0$ dB, the condition for a transceiver pair to be connected is that the received signal strength is greater than the interference power. Thus, for $\Theta \geq 1$, the cardinality of the transmitting set can at most be one, and that transmitter is the one with the best channel to the receiver. The following proposition forms the basis of the estimation algorithm.

Proposition 5.2: Under the conditions of Rayleigh fading and $N_0 \ll I$, the cardinality of the transmitting set is well-approximated by a Poisson distribution with parameter $(\Gamma(1+2/\gamma)\Gamma(1-2/\gamma)\Theta^{2/\gamma})^{-1}$.

Proof: Extending the procedure used for deriving (26), we see that the success probability for a transceiver pair at an arbitrary distance R units apart is

$$p_s(R) = c_1'(R)\exp(-c_2 R^2),$$

where $c_1'(R) = \exp(-N_0 R^\gamma \Theta)$. For $N_0 \ll I$, $p_s \approx \exp(-c_2 R^2)$. Now, we place an additional receiver node O at the origin (which does not affect the distribution of the PPP) and analyze the transmitting set for this "typical" node.

Consider a disc of radius a centered at the origin. Let E_i denote the event that the ith transmitter inside this disc is in O's transmitting set. For R uniformly distributed in $[0, a]$, we have

$$\begin{aligned} \mathbb{P}(E_i) &= \mathbb{E}_R[p_s(R) \mid R] \\ &= \frac{2\pi}{\pi a^2} \int_0^a r e^{-c_2 r^2} dr \\ &= \frac{1}{a^2 c_2}(1 - e^{-a^2 c_2}). \end{aligned} \tag{32}$$

Note that in any given time slot, the events E_i and E_j for arbitrary transmitters i and j are actually slightly correlated. This is because i acts as an interferer for j's signal and vice versa. We neglect this minor dependence and assume that the E_i's are independent events. Also, since $\mathbb{P}(E_i)$ is independent of i, we take $\mathbb{P}(E_i) = \mathbb{P}(E)$, $\forall i$, to simplify notation. Denote the mean number of transmitters in the disc of radius a by $N_a = \lambda p \pi a^2$. Then, the probability of having exactly k elements in the transmitting set T is calculated as

$$\begin{aligned}
\mathbb{P}(N_T = k) &= \lim_{a\to\infty} \mathbb{E}_{N:N\geq k}\left[\binom{N}{k}\mathbb{P}(E)^k(1-\mathbb{P}(E))^{N-k}\right] \\
&= \lim_{a\to\infty} \sum_{n=k}^{\infty} \frac{e^{-N_a}N_a^n}{n!}\binom{n}{k}\mathbb{P}(E)^k(1-\mathbb{P}(E))^{n-k} \\
&\overset{(a)}{=} \lim_{a\to\infty} \frac{(\mathbb{P}(E)N_a)^k}{k!}\sum_{s=0}^{\infty}\frac{e^{-N_a}N_a^s}{s!}\cdot(1-\mathbb{P}(E))^s \\
&= \lim_{a\to\infty} \frac{(\mathbb{P}(E)N_a)^k}{k!}\exp(-N_a\mathbb{P}(E)) \\
&= \exp(-c_4)c_4^k/k!, \qquad (33)
\end{aligned}$$

where (a) is obtained on using the substitution $n-k=s$, and $c_4 = \lim_{a\to\infty} N_a\mathbb{P}(E) = 1/(\Gamma(1+2/\gamma)\Gamma(1-2/\gamma)\Theta^{2/\gamma})$. □

Therefore, the cardinality of the transmitting set, N_T, is distributed as a Poisson random variable with mean c_4, and is, surprisingly, independent of λ and p. Because of the homogeneity in the nodal arrangement, the size of each node's transmitting set obeys the same statistics. Fig. 8 plots the theoretic expected size of the transmitting set $\bar{N}_T$ for different threshold values at various PLE values.

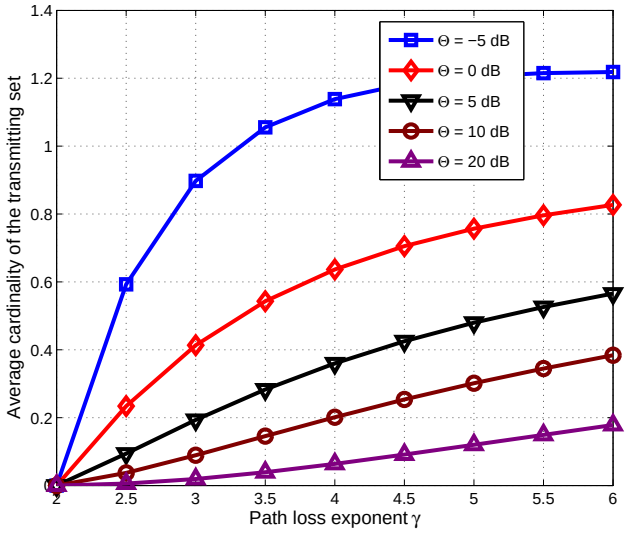

Fig. 8. The mean number of elements in the transmitting set versus γ for different SIR threshold values.

Comparing the empirical mean cardinality of the transmitting set to c_4, γ can be estimated using a look-up table. Alternatively, we may use a differential method where we measure the mean cardinalities of the transmitting sets for two different values of Θ, Θ_1 and Θ_2. Denote the mean transmitting set sizes corresponding to the two values of Θ as $\bar{N}_T^1$ and $\bar{N}_T^2$. Theoretically, we obtain

$$\frac{\bar{N}_T^1}{\bar{N}_T^2} = \left(\frac{\Theta_2}{\Theta_1}\right)^{2/\gamma},$$

giving us an unbiased estimate as

$$\hat{\gamma} = \frac{2\ln(\Theta_2/\Theta_1)}{\ln(\bar{N}_T^1/\bar{N}_T^2)}. \tag{34}$$

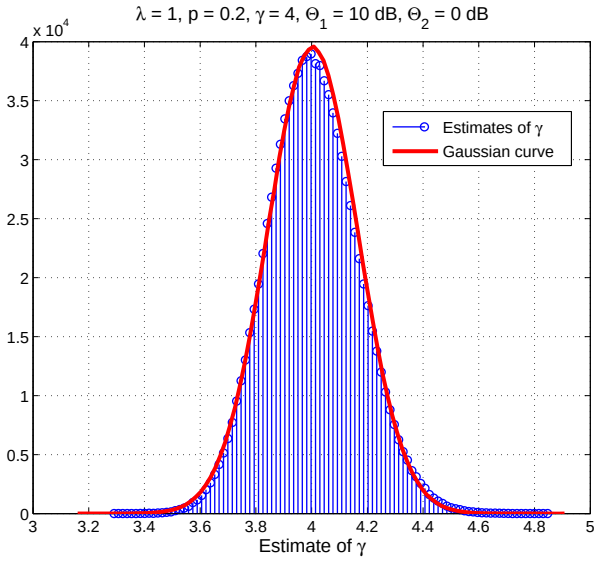

Fig. 9. Histogram of $\hat{\gamma}$ for the estimation algorithm based on the cardinality of the transmitting set. Error variance ≈ 0.03.

Fig. 9 plots the histogram of the estimated PLE values when the actual value is $\gamma = 4$. The estimation error for this scheme also seems approximately Gaussian.

We now analytically evaluate the Crámer-Rao lower bound for an unbiased estimate of N_T. From (33), we have

$$\ln f(N_T = k;\gamma) = -c_4 + k\ln(c_4) - \ln(k!) \tag{35}$$

The Fisher information for an unbiased estimate of γ is then given by

$$\begin{aligned} J(\gamma) &= \mathbb{E}_{N_T}\left[-\frac{\partial^2}{\partial\gamma^2}\ln f(N_T;\gamma)\right] = \frac{1}{c_4}\left(\frac{\partial c_4}{\partial\gamma}\right)^2 \\ &= \frac{4\left[\psi(1-\frac{2}{\gamma}) - \psi(1+\frac{2}{\gamma}) - \ln(\Theta)\right]^2}{\gamma^4\Gamma(1+\frac{2}{\gamma})\Gamma(1-\frac{2}{\gamma})\Theta^{\frac{2}{\gamma}}}, \end{aligned} \tag{36}$$

where $\psi(x)$ represents the digamma function[5] and has the integral representation

$$\psi(x) = \int_0^\infty \left(\frac{e^{-t}}{t} - \frac{e^{-xt}}{1-e^{-t}} \right) dt.$$

We have CRLB $= 1/J(\gamma)$.

b) Error Analysis when the fading distribution is not necessarily Rayleigh: The method based on the cardinality of the transmitting set assumes that channel is Rayleigh-faded. It is interesting to see how large the error is when the true value of m is not 1. We now derive some analytical results showing the dependence of the algorithm on the fading parameter m. Specifically, we determine the distribution of N_T for integer values of m and comment on its effect on the estimation algorithm.

When G is a Nakagami-m distributed variable, we can generalize (31) to obtain the success probability for a transceiver pair at an arbitrary distance R units apart as

$$p_s(R) = \sum_{k=0}^{m-1} \frac{\exp(-c_3 R^2) \left(c_3 R^2\right)^k}{k!} \left(\frac{2}{\gamma}\right)^k, \quad m \in \mathbb{Z}^+. \tag{37}$$

Using this, we obtain

$$\begin{aligned}
\mathbb{P}(E) &= \mathbb{E}_R[p_s(R) \mid R] \\
&= \frac{2\pi}{\pi a^2} \int_0^a \sum_{k=0}^{m-1} \frac{\exp(-c_3 r^2) r^{2k}}{k!} \left(\frac{2c_3}{\gamma}\right)^k r dr \\
&= \frac{1}{a^2} \sum_{k=0}^{m-1} \left(\frac{2c_3}{\gamma}\right)^k \int_0^a \frac{\exp(-c_3 r^2)}{k!} r^{2k} 2r dr \\
&\overset{(a)}{=} \frac{1}{a^2 c_3} \sum_{k=0}^{m-1} \left(\frac{2}{\gamma}\right)^k \frac{1}{k!} \int_0^{c_3 a^2} t^k \exp(-t) dt \\
&\overset{(b)}{=} \frac{1}{a^2 c_3} \sum_{k=0}^{m-1} \left(\frac{2}{\gamma}\right)^k \frac{1}{k!} \left(1 - \Gamma(k+1, c_3 a^2)\right),
\end{aligned} \tag{38}$$

where (a) is obtained by a simple change of variables ($t = c_3 r^2$) and (b) using the definition of the incomplete gamma function. Following the steps used in the derivation of (33), the cardinality of the transmitting set is seen

[5]Mathematica: PolyGamma[x]

to be Poisson distributed with mean c_5, where

$$\begin{aligned} c_5 &= \lim_{a\to\infty} N_a \mathbb{P}(E) \\ &\overset{(a)}{=} \frac{\lambda p \pi}{c_3} \sum_{k=0}^{m-1} \left(\frac{2}{\gamma}\right)^k \\ &= \frac{\lambda p \pi}{c_3} \frac{1-\left(\frac{2}{\gamma}\right)^m}{1-\frac{2}{\gamma}} \\ &\overset{(b)}{=} \frac{\Gamma(m)\left(1-\left(\frac{2}{\gamma}\right)^m\right)}{\Gamma(m+\frac{2}{\gamma})\Gamma(2-\frac{2}{\gamma})\Theta^{2/\gamma}}. \end{aligned} \tag{39}$$

Here, (a) is obtained using the fact that $\lim_{z\to\infty}\Gamma(a,z)=\Gamma(a)$ and (b) using the definition of c_3 and [13, Eqn. 17]

$$\mathbb{E}[G^{2/\gamma}] = \frac{\Gamma(m+2/\gamma)}{\Gamma(m)m^{2/\gamma}}.$$

The analytical value of the mean cardinality of the transmitting set when $m \in \mathbb{Z}^+$ is plotted in Fig. 10 for two different thresholds.

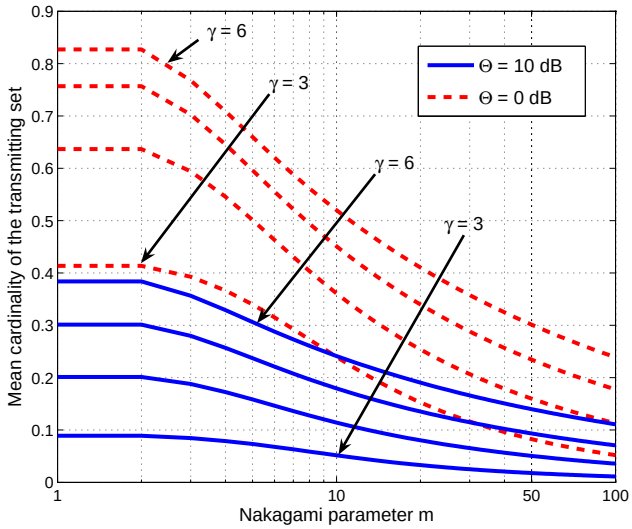

Fig. 10. The expected cardinality of the transmitting set for various values of γ.

From (39), we see that $\bar{N}_T$ is inversely proportional to $\Theta^{2/\gamma}$. Therefore, if we use a differential method to estimate γ, we still obtain

$$\frac{\bar{N}_T^1}{\bar{N}_T^2} = \left(\frac{\Theta_2}{\Theta_1}\right)^{2/\gamma}.$$

Remarkably, when m is a positive integer, it has no effect on the performance of the algorithm. Based on this observation, we surmise that the behavior of the error is independent of m, even when $m \notin \mathbb{Z}$. Fig. 11 plots the

empirical MSE for the differential method, taken over several different network realizations versus m for various PLE values. As expected, the MSE is insensitive to the fading parameter.

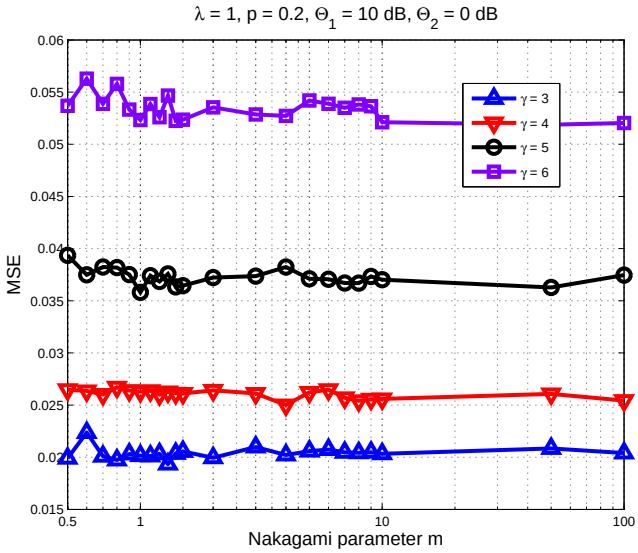

Fig. 11. The value of the MSE versus m for different PLEs.

VI. Comparison of the Algorithms

In this section, we compare the features of the three algorithms for PLE estimation described in the earlier section. A common characteristic of all the algorithms are that the estimation errors are (roughly) Gaussian, since the histogram of the errors fit well into normal distribution curves. Furthermore, the differential algorithms are seen to be accurate and do not require estimates of λ or the contention probability p.

1) The method that predicts γ using the knowledge of the interference moments can also be used to estimate p and m. It is seen to work well for a wide range of system parameters and importantly is accurate independent of the value of m. Though it is fairly simple in principle, it invokes a scheduling procedure for taking measurements, since all the nodes inside the guard zone are required to stop transmitting.
2) The scheme that estimates γ upon calculating outage probabilities does not need a guard zone to be imposed, but requires a transmitter that originally did not belong to the process to be placed at unit distance from the receiver. Moreover, it is formalized only for the Rayleigh fading case ($m = 1$). The error is seen to be high when fading is severe (values of m lower than 1), and more so when the PLE is high. Also, this algorithm is convenient to use only when the network is interference-limited, i.e., the noise level is considerably lower than the interference power.
3) The algorithm based on the connectivity properties of the PPP does not need any node location information or the imposition of a guard zone around the nodes. Furthermore, it is robust in the sense that it performs

independently of the value of the fading parameter m. Like the previous algorithm, it is, however, based on the condition that the system is interference-limited.

We now address a couple of performance issues related to the rate of convergence of the algorithms. First, the success of these methods is critically determined by the number of survey points N to be taken. A small value of N will result in low accuracy while a large value of N will result in an expensive survey process with many of the survey points giving little benefit. The second aspect is related to centralized versus distributed information processing. Specifically, the efficiency of these techniques relies on how the nodes that take measurements are chosen. Consider the two extreme cases where nodes $1, 2, \ldots N$ can be chosen in a random fashion or as subsequent nearest neighbors. In the latter method, the first node relays its measurement information to its nearest neighbor which then passes this on along with its own measured value, to its nearest neighbor other than the first node, and information is propagated in this manner. If nodes are chosen this way in a local fashion, the measurements will be correlated and the algorithm takes a long time to converge. On the other hand, choosing nodes randomly may result in choosing nodes sufficiently far apart but will also incur a lot of overhead when information needs to be exchanged between nodes or relayed to a central server or a fusion center.

Fig. 12 compares the performance of the three algorithms. Here, R refers to the centralized computing scheme where measurements are taken at randomly picked nodes and relayed to the central server, while NN refers to the distributed algorithm where measurements are passed over to subsequent nearest neighbors. From the plot, we see that the algorithm based on the interference moments clearly has the lowest MSE. Also, for the first two schemes, choosing randomly located nodes for measurements leads to a much faster convergence than when choosing subsequent nearest neighbors. However, for the method based on the cardinality of the transmitting set, the order in which nodes are picked does not have a huge impact on its convergence rate.

Our algorithms work well even with more general point process models. We tested them for networks with two other forms of nodal distribution, the Matern hard core process and the Thomas clustered process [15], and the estimated PLE values are seen to accurately match the true values.

Finally, we remark that in reality, the PLE value changes depending on the terrain category and the environmental conditions, and hence cannot always be assumed to be a constant over the entire network. However, our algorithms are still useful since they can be used for obtaining local estimates, based on measurements taken over neighborhoods. For cases where the channel behavior is different for different regions of the network, it can be divided into sub-areas with constant γ that are analyzed separately.

VII. Conclusion

In wireless systems, the value of the PLE is critical but not known a priori, thus an accurate estimate is essential for the analysis and design of systems. We offer a novel look at the issue of PLE estimation in a large wireless

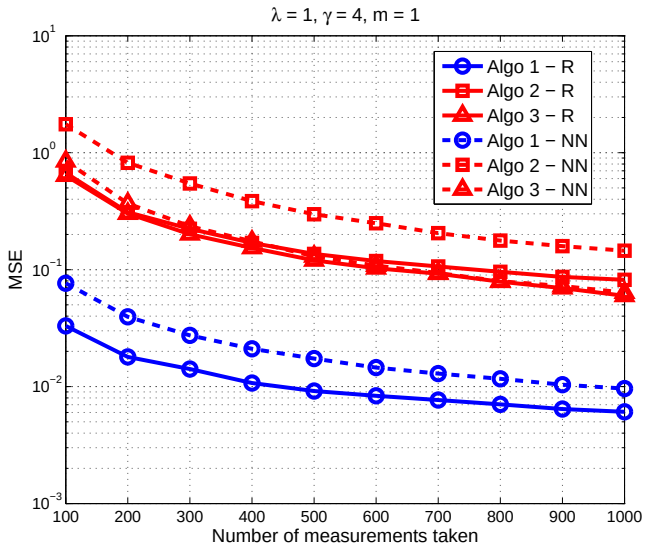

Fig. 12. Comparison of the MSE performance of the three algorithms.

network, by taking into account Nakagami-m fading, the underlying node distribution and the network interference. Nodes are assumed to be arranged as a homogeneous PPP on the plane and the channel access scheme is slotted ALOHA. For such a system, the paper describes three separate algorithms for PLE estimation. Simulation results are provided to demonstrate their performance and quantify the estimation errors. For each of the algorithms, we find that the estimation error is approximately Gaussian. Comparing the algorithms, we see that the one that is based on the interference moments performs the best in terms of minimizing the MSE. We also provide methods to infer the intensity of the PPP and evaluate Crámer-Rao lower bounds on the MSE.

REFERENCES

[1] T. S. Rappaport, *Wireless Communications - Principles and Practice*, Prentice Hall, 1991.

[2] W. C. Jakes, "Microwave Mobile Communications," Wiley-IEEE Press, May 1994.

[3] A. Savvides, W. L. Garber, R. L. Moses and M. B. Srivastava, "An Analysis of Error Inducing Parameters in Multihop Sensor Node Localization," *IEEE Transactions on Mobile Computing*, Vol. 4, No. 6, pp. 567-577, Nov./Dec. 2005.

[4] N. Patwari, I. Hero, A. O. M. Perkins, N. Correal, and R. ODea, "Relative Location Estimation in Wireless Sensor Networks," *IEEE Transactions on Signal Processing*, Vol. 51, No. 8, pp. 2137-2148, Aug. 2003.

[5] C. Bettstetter, "On the Connectivity of Ad Hoc Networks," *The Computer Journal, Special Issue on Mobile and Pervasive Computing*, Vol. 47, No. 4, pp. 432-447, July 2004.

[6] D. Miorandi and E. Altman, "Coverage and Connectivity of Ad Hoc Networks in the Presence of Channel Randomness," *IEEE INFOCOM*, Mar. 2005.

[7] A. Özgür, O. Lévêque and D. Tse, "Hierarchical Cooperation Achieves Optimal Capacity Scaling in Ad Hoc Networks," *IEEE Transactions on Information Theory*, Vol. 53, No. 10, pp. 3549-3572, Oct. 2007.

[8] M. Sikora, J. N. Laneman, M. Haenggi, D. J. Costello, Jr., and T. E. Fuja, "Bandwidth- and Power-Efficient Routing in Linear Wireless Networks," *IEEE Transactions on Information Theory*, Vol. 52, No. 6, pp. 2624-2633, June 2006.

[9] M. Haenggi, "On Routing in Random Rayleigh Fading Networks," *IEEE Transactions on Wireless Communications*, Vol. 4, No. 4, pp. 1553-1562, July 2005.

[10] J. Venkataraman, M. Haenggi and O. Collins, "Shot Noise Models for Outage and Throughput Analyses in Wireless Ad Hoc Networks," *Military Communications Conference* (MILCOM'06), Washington DC, Oct. 2006.

[11] F. Baccelli, B. Błaszczyszyn and P. Mühlethaler, "An Aloha Protocol for Multihop Mobile Wireless Networks," *IEEE Transactions on Information Theory*, Vol. 52, No. 2, pp. 421-436, Feb. 2006.

[12] G. Mao, B. D. O. Anderson and B. Fidan, "Path Loss Exponent Estimation for Wireless Sensor Network Localization," *Computer Networks*, Vol. 51, Iss. 10, pp. 2467-2483, July 2007.

[13] M. Nakagami, *The m-distribution : A General Formula for Intensity Distribution of Rapid Fading*, in W. G. Hoffman, "Statistical Methods in Radiowave Propagation," Pergamon Press, Oxford, U. K., 1960.

[14] S. M. Kay, "Fundamentals of Statistical Signal Processing, Volume I: Estimation Theory," Prentice Hall, Mar. 1993.

[15] D. Stoyan, W. S. Kendall and J. Mecke, "Stochastic geometry and its applications," Wiley & Sons, 1978.

[16] Edwin L. Crow; Robert S. Gardner, "Confidence Intervals for the Expectation of a Poisson Variable," *Biometrika*, Vol. 46, No. 3/4, pp. 441-453, Dec. 1959.

[17] M. Haenggi, "On Distances in Uniformly Random Networks," *IEEE Transactions on Information Theory*, vol. 51, pp. 3584-3586, Oct. 2005.

[18] S. Srinivasa and M. Haenggi, "Modeling Interference in Finite Uniformly Random Networks," *International Workshop on Information Theory for Sensor Networks (WITS '07)*, Santa Fe, June 2007.